Biointerface Research in Applied Chemistry
Platinum Open Access Journal (ISSN: 2069-5837)

*Article*
**Volume 12, Issue 1, 2022, 49 - 60**
https://doi.org/10.33263/BRIAC121.049060

# Antitumor Activities of Co-loading Gemcitabine and Oxaliplatin into Oleic Acid-Based Solid Lipid Nanoparticle against Non-Small Cell Lung Cancer Cells

**Ashwaq A. Al-Mutairi [1], Mayson H. Alkhatib [1,2,*], Hana M. Gashlan [1,*]**

[1] Department of Biochemistry, Faculty of Science, King Abdulaziz University, Jeddah, Saudi Arabia
[2] Regenerative Medicine Unit, King Fahd Medical Research Center, King Abdulaziz University, Jeddah, Saudi Arabia
* Correspondence mhalkhatib@kau.edu.sa;

Scopus Author ID 26436355800
**Received: 13.03.2021; Revised: 5.04.2021; Accepted: 8.04.2021; Published: 19.04.2021**

**Abstract:** Lung cancer is a main global health problem with high incidence and case-fatality rates. The use of solid lipid nanoparticles (SLN) as a nanocarrier for chemotherapeutic agents has been suggested as an effective therapeutic approach. The current work objective was to investigate the antineoplastic activity of gemcitabine (GM) and oxaliplatin (OXA) co-loaded into oleic acid-based solid lipid nanoparticle (OA-SLN) in A549 non-small cell lung cancer cells. OA-SLN was synthesized using homogenization and physically characterized using the dynamic light scattering techniques. The anticancer properties of the combination of GM and OXA encapsulated in OA-SLN were evaluated using a series of cellular assays, such as cell viability using crystal violate, apoptosis using caspase-3 assay kit, and autophagy using human autophagy-related protein LC3-B ELISA kit. The z-average diameter of (GM+OXA) OA-SLN was (63.10 ± 1.53 nm). The (GM+OXA) OA-SLN formulation had significantly reduced cell growth in a dose-dependent manner on the A549 cells within 24 hours. The combination (GM+OXA) OA-SLN had more pronounced effects on autophagy (326.38 ± 4.21 pg/ml) than the untreated control cells (206.2 ± 6.69 pg/ml). Our findings indicate that co-encapsulation of GM and OXA into OA-SLN significantly improved their therapeutic efficacy against A549 cells.

**Keywords:** chemotherapeutic agents; apoptosis; A549 cell line; nanocarrier; autophagy; cytotoxicity.



## 1. Introduction

Lung cancer is a deadly adult cancer that is responsible for the most cancer deaths worldwide [1]. Non-Small Cell Lung Carcinoma (NSCLC) is the most widespread form and accounts for more than 80% of all cases [2]. Conventional treatment choices, including surgery, radiotherapy, immunotherapy, and chemotherapy, are the main therapy regimens for lung cancers [3]. However, over half of NSCLC patients have developed metastases at the time of diagnosis, and only ~14% have 5-year survival [4]. Hence, there is an urgent need to develop novel treatment strategies to combat this disease.

Combination therapy has gained attention in cancer treatment because drugs can act through different pathways and offer the possibility of synergistic effects, thus minimizing induced drug toxicities associated with a higher dose of individual drugs [5]. In this study, two anticancer drugs, namely gemcitabine (GM) and oxaliplatin (OXA), were selected to treat NSCLC cells. GM, a pyrimidine nucleoside antimetabolite, has an established and significant role in treating various types of human cancers, including lung cancer [6]. However, GM has

many drawbacks, including a lack of tumor specificities, leading to high toxicity and low therapeutic outcome [7]. Also, GM has a short half-life due to its small molecular weight and high hydrophilicity and is rapidly decomposed into inactive products after administration [8]. OXA, third-generation platinum-based anticancer drug, acts by interfering with the DNA replication machinery and forms the DNA adducts [9, 10]. But, its low water solubility, short half-life, and lack of selective biodistribution reduces the effectiveness of OXA in the targeted tissues and increase the systemic toxicity [11]. The design of nanocarriers for GM and OXA delivery is one strategy to overcome their limitations and improve their efficacy in NSCLC treatment.

Nanocarriers have attracted much recent interest in treating lung cancers because of their ability to improve drug delivery toward specific biological targets to achieve safer and more effective therapy [3]. A drug's encapsulation into a nanocarrier might also prevent its deactivation by other biomolecules, high drug loading capability, and enhance its bioavailability and stability [12].

Solid lipid nanoparticles (SLNs) have arisen as potential nanocarriers for drug delivery systems with a mean particle size range between 50 and 1000 nm. They consist of a solid lipophilic matrix at body temperature, in which biologically active substances can be dissolved or entrapped [13]. Moreover, SLNs have many advantages: control drug release, promote oral absorption of drugs, modify the pharmacokinetics and pharmacodynamics, enhance tissue or cell-specific targeting, adjust tissue distribution, and reduce side effects [14].

Oleic acid (OA) is an omega-9 monounsaturated fatty acid characterized by potent cytotoxic activity [15]. Entrancingly, it is selectively cytotoxic to malignant cells without affecting the healthy ones [16]. Hence, OA was selected as an ideal agent to prepare the novel SLN. Also, cholesterol (CH) and phosphatidylcholine (PC) were selected as amphipathic lipids in the formula because of their ability to increase SLN stability and decrease toxicity [17].

In the present study, our goal was to design a novel OA-based SLN for delivering GM and OXA into the NSCLC to increase efficacy and decrease the side effects. The physical characteristics and *in vitro* antitumor activities against A549 cells of the OA-based SLN and (GM+OXA) OA-SLN were investigated.

## 2. Materials and Methods

### *2.1. Materials.*

Oleic acid (OA) was purchased from BDH Chemicals Ltd (Poole, England), and Tween 80 (T80) was obtained from Al Shafei Medical and Scientific Equipment Est. (Jeddah, KSA). PC was purchased from Sigma-Aldrich (Germany), and CH was obtained from Techno Pharmchem (India). OXA and GM were gifted from King Abdulaziz University Hospital (Jeddah, KSA). Crystal violet was purchased from S D Fine-Chem Ltd. (Mumbai, India). Caspase-3 assay kit was purchased from BioAssay Systems (Hayward, USA). Human autophagy-related protein LC3-B ELISA kit was purchased from Sunlong Biotech Co., Ltd (Hangzhou, China). All other chemicals were of reagent grade and used without further modifications.

### *2.2. Synthesis of OA-based SLN.*

OA-SLN was produced by homogenization method in which the aqueous phase and lipid phase were separately prepared. First, the aqueous phase was formed by dissolving OA

and T80 in 10 mL of buffer followed by heating to above 80°C. Simultaneously, in another flask, the solid lipid phase was produced by mixing the PC and CH at the molten state (80°C). Second, the aqueous phase was added to the lipid phase dropwise to produce a solution with an incessant mixing. After that, the solution was immediately homogenized at 13,000 rpm for 30 min and stored at 25°C.

*2.3. Preparation of GM and OXA encapsulated OA-SLN.*

The stock solutions were prepared by dissolving 1 mg of GM into 1 mL of OA-SLN formula (GM OA-SLN). Similarly, the stock solution of 1 mg/mL of GM-SOL was produced by dissolving GM in distilled water. The stock solutions of OXA were prepared by combining 100 µL of 5 mg/mL of OXA with 100 µL of SLN (OXA OA-SLN). Also, the stock solution of OXA-SOL was prepared by dissolving 100 µL of 5 mg/mL of OXA directly to the water. The drug-loaded SLN was stored in the refrigerator until further use. All of the serial dilutions of the produced formulas were performed using the culture media.

*2.4. Physical characterization of OA-SLN.*

The average size diameter, zeta potential, and the polydispersity index (PDI) of blank OA-SLN, GM OA-SLN, OXA OA-SLN, and (GM+OXA) OA-SLN samples were quantified at 25 ± 0.2 °C by the Zetasizer (3000 HS, Malvern Instruments, Malvern, UK) using dynamic light scattering method.

*2.5. Cell cultures.*

The A549 non-small cell lung cancer cell line was obtained from King Abdulaziz University Hospital (Jeddah, KSA). Cells were preserved in Dulbecco's modified Eagle's medium containing 10% fetal bovine serum and antibiotics (100 mg/mL streptomycin, 100 U/mL penicillin) and were grown in 5% $CO_2$, at 37°C.

*2.6. Cytotoxicity screening using crystal violate assay.*

The effect of OA-SLN, GM OA-SLN, and OXA OA-SLN on the viability of A549 cells was measured using crystal violate assay. Briefly, A549 cells ($1\times10^5$ cells/well) were cultured onto 96-well plates and incubated overnight. Cells were then treated with 100 µL of varying dosing levels of blank OA-SLN, GM OA-SLN, OXA OA-SLN, and (GM+OXA) OA-SLN besides their matching solution formulas that replace the SLN with water (n = 3) for 24 h at 37 °C in a $CO_2$ incubator. The cell viability was measured by adding 50 µL of crystal violate reagent followed by 10 min incubation at 25°C. Afterward, the 96-well plate was washed two times with tap water, followed by adding 100 µL of 1% Sodium dodecyl sulfate to solubilize the stain. The absorbance (A) was measured using a microplate reader (BioTek, US) at 570 nm. Wells with untreated cells were used as control positive, and wells included culture media (blank) considered as negative controls. The percentages of cell viabilities were calculated by the following equation:

$$\text{Cell viability (\%)} = \frac{(\text{A of treated cell} - \text{A of blank})}{(\text{A of control} - \text{A of blank})} \times 100$$

*2.7. Characterization of cell morphology of A549 cells.*

The effect of selected treatment of blank OA-SLN, GM OA-SLN, OXA OA-SLN, and (GM+OXA) OA-SLN and their matching solution formulas on the morphological changes of A549 cell line was assessed as elaborated by Alkhatib *et al.* (2020) [18]. Briefly, A549 cells were fixed and stained with 0.02 % Coomassie Blue dye to observe their morphological changes using a phase-contrast inverted light microscope (Olympus, Japan). Untreated cells were used as a control.

*2.8. Apoptotic effect assessment using DAPI stain.*

The apoptosis effects of the tested formulas of the blank OA-SLN, GM OA-SLN, OXA OA-SLN, and (GM+OXA) OA-SLN and their solution were evaluated by DAPI staining for the A549 cells as mentioned by Alkhatib *et al.* (2018) [19]. Untreated (control) and treated A549 cells were stained with 300 nM of DAPI, a DNA stain attached to A-T regions of dsDNA and emitted blue fluoresces, resulting in displaying the nuclear changes in the cells under the fluorescent microscope (Leica CRT6000, Germany).

*2.9. Measurement of caspase-3 activity.*

A549 cell apoptosis was evaluated by measuring the activity of caspase-3 using a caspase-3 assay kit. In brief, each well in a 96-well plate was seeded with 5000 A549 cells and incubated for 24 h. After that, cells were treated with 100 µL of different dosing levels of blank OA-SLN, GM OA-SLN, OXA OA-SLN, and (GM+OXA) OA-SLN besides their matching solution formulas (n = 2) and were re-incubated for 24 h at 37 °C in a CO2 incubator. Then, the activity of caspase-3 was measured in the A549 cancer cells using a kit from BioAssay Systems as illustrated by the manufacturer's instructions. The fluorescence intensity examined using a Synergy HT microplate reader (BioTek, US) at excitation/emission wavelengths of 360/460-nm.

*2.10. Autophagy assessment.*

Microtubule-associated protein 1A/1B-light chain 3 (LC3-B) is widely used as a marker of autophagy because it is present in autophagosomes [20]. In general, A549 cells (25000 cells/well) seeded in 24-well plates were treated with the desired formula (n = 2) for 24 h. After treatment, cell lysate was assessed for the concentrations of LC3-B using a human autophagy-related protein LC3-B ELISA kit as mentioned by the manufacturer's instructions. The absorbance was measured at 450 nm using a Synergy HT microplate reader (BioTek, US).

*2.11. Statistical analyses.*

All assays were conducted in triplicate unless and otherwise mentioned in the reported method section. The results were expressed as mean ± standard deviation (SD). All the experimental data were compared using the one-way analysis of variance (ANOVA) test using the MegaStat Excel (version 10.3, Butler University, Indianapolis, IN). A P-value < 0.05 was considered a statistically significant difference between the tested samples.

## 3. Results and Discussion

*3.1. Characteristics of OA-SLN.*

OA-SLN and drug encapsulated OA-SLN (GM OA-SLN, OXA OA-SLN, and (GM+OXA) OA-SLN)) were prepared and characterized by measuring the particle size, zeta potential, and PDI by dynamic light scattering (Figure 1). As shown in Figures 1A and 1B, all formulas had small particle sizes ranged from 63 to 200 nm and had a negative surface charge. Most importantly, (GM+OXA) OA-SLN were significantly smaller in size (63.10 ± 0.88) nm compared to single drug encapsulated OA-SLN. Additionally, all formulas' PDI was lower than 1, and OXA OA-SLN had the lowest PDI (0.25 ± 0.02) (Figure 1C).

*3.2. In vitro cytotoxicity studies.*

The cytotoxic influence of the solution formulas (GM-SOL, OXA-SOL, and (GM+OXA)-SOL), and the SLN formulas (GM OA-SLN, OXA OA-SLN and (GM+OXA) OA-SLN) on A549 lung cancer cells was determined using crystal violate assay (Figure 2). GM and OXA, either loaded in water or SLN, were evaluated at concentrations ranging from 3.125 to 100 µM. The results showed that GM OA-SLN and OXA OA-SLN showed a dose-dependent cytotoxic efficacy on the A549 cells within 24 h. Moreover, OA-SLN significantly increased GM and OXA inhibition on the proliferation of A549 cells in all concentrations (Figure 2 (A, B)). The $IC_{50}$ value of GM OA-SLN (67.26 ± 2.10) µM was somewhat lesser than that of free GM solution (70.91± 3.20) µM in 24 h treatment, whereas the $IC_{50}$ value of OXA OA-SLN (5.28 ± 1.02) µM was considerably lower compared with free OXA solution (44.81 ± 2.03) µM in 24 h treatment. These results indicated that GM and OXA loaded OA-SLN had a considerable antiproliferation effect on carcinoma cells than free GM and OXA solution *in vitro*.

Better therapeutic outcomes for resistant tumor cells were mainly achieved via combinational therapy based on two or more anticancer agents. Furthermore, the combined doses of GM and OXA loaded into OA-SLN were determined and compared with a relative amount of (GM+OXA)-SOL when subjected to A549 cells for 24 h. As summarized in Figure 2C, (GM+OXA) OA-SLN exhibited a lower $IC_{50}$ value at ratio 1:4 of GM to OXA, respectively, when compared to (GM+OXA)-SOL which had $IC_{50}$ at ratio 1:0.5 of GM to OXA, respectively. It was clearly observed that (GM+OXA) OA-SLN had a significant superior cytotoxic activity on A549 cells compared to free (GM+OXA)-SOL mixture.

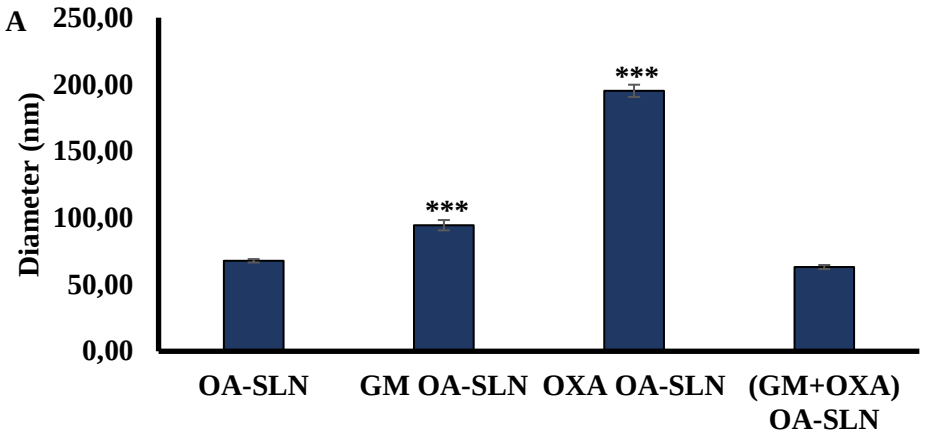

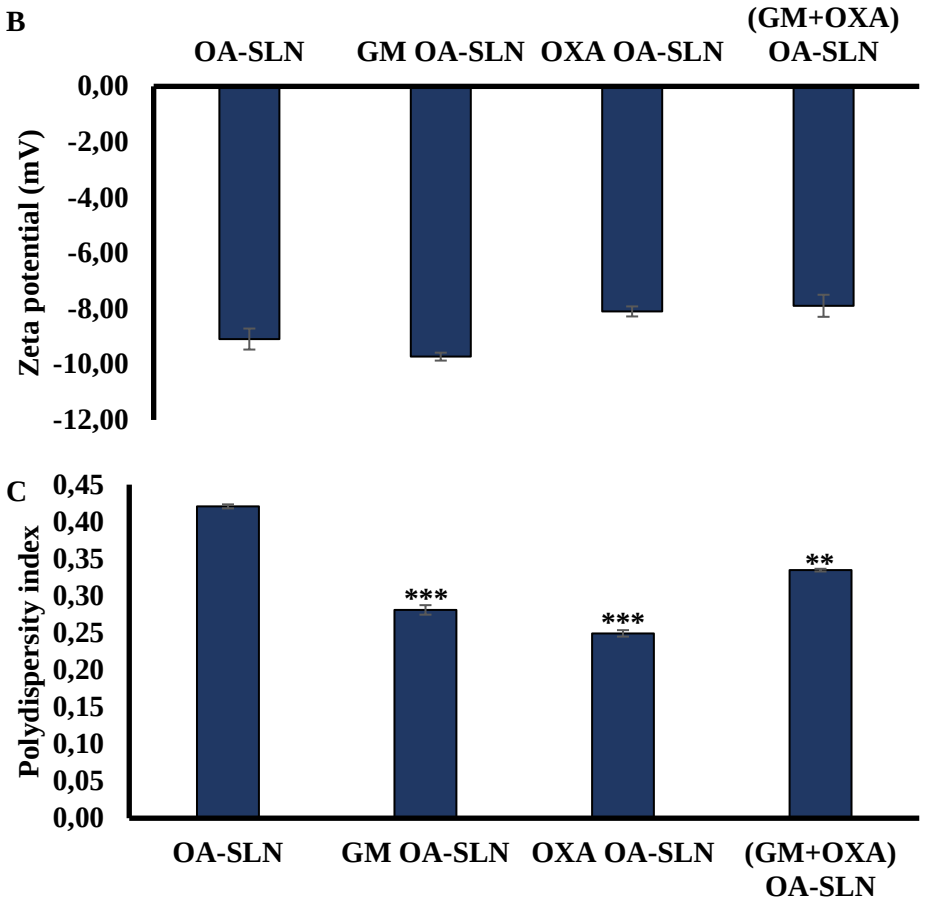


**Figure 1.** Physical characteristics of OA-SLN formulas in terms of (**A**) Size; (**B**) Zeta potential; (**C**) Polydispersity index. * = p < 0.05, ** = p < 0.01, *** = p < 0.001 display the significant differences between OA-SLN and the desired drug-loaded OA-SLN formula. Data represent mean ± SD of three experiments.

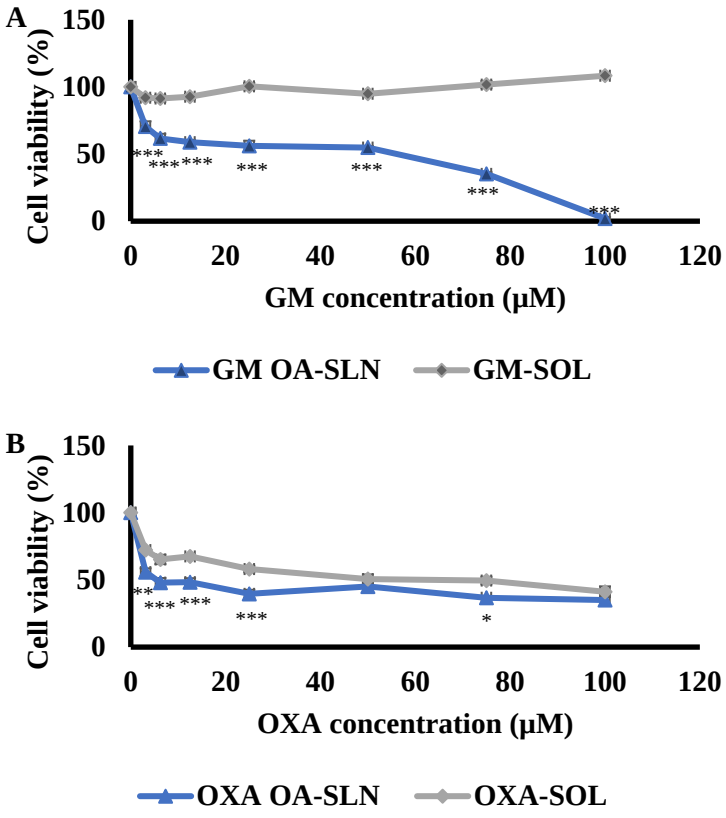

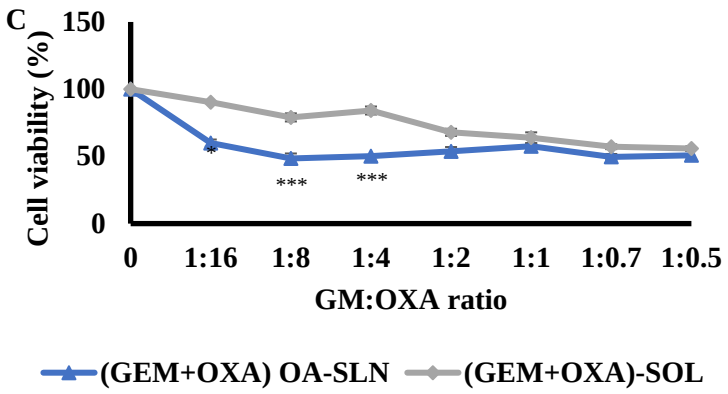


**Figure 2.** *In vitro* cytotoxicity effect of solution formulas and SLN formulas at different concentrations on the % cell viabilities of A549 NSCLC cells after 24 h treatment. (**A**) GM OA-SLN versus GM-SOL; (**B**) OXA OA-SLN versus OXA-SOL; (**C**) (GM+OXA) OA-SLN vs (GM+OXA)-SOL. Data represent mean ± SD of three experiments. * = $p < 0.05$, ** = $p < 0.01$, *** = $p < 0.001$ display the significant differences between SLN-formula and SOL-formula.

*3.3. Morphological examination of A549 cells.*

As demonstrated in Figure 3, A549 cells showed morphological changes after treatment for 24 h. All treated A549 cells with nanoparticles (OA-SLN, GM OA-SLN, OXA OA-SLN, and (GM+OXA) OA-SLN) have revealed late signs of apoptosis as their size has enlarged and membrane blebbing with collapse nucleus were seen whereas cells treated with SOL-formula their shape were altered. Also, cells treated with all tested formulas displayed an increase in the intercellular spaces between cells; however, it was more significant in cells treated with all OA-SLN formulas.

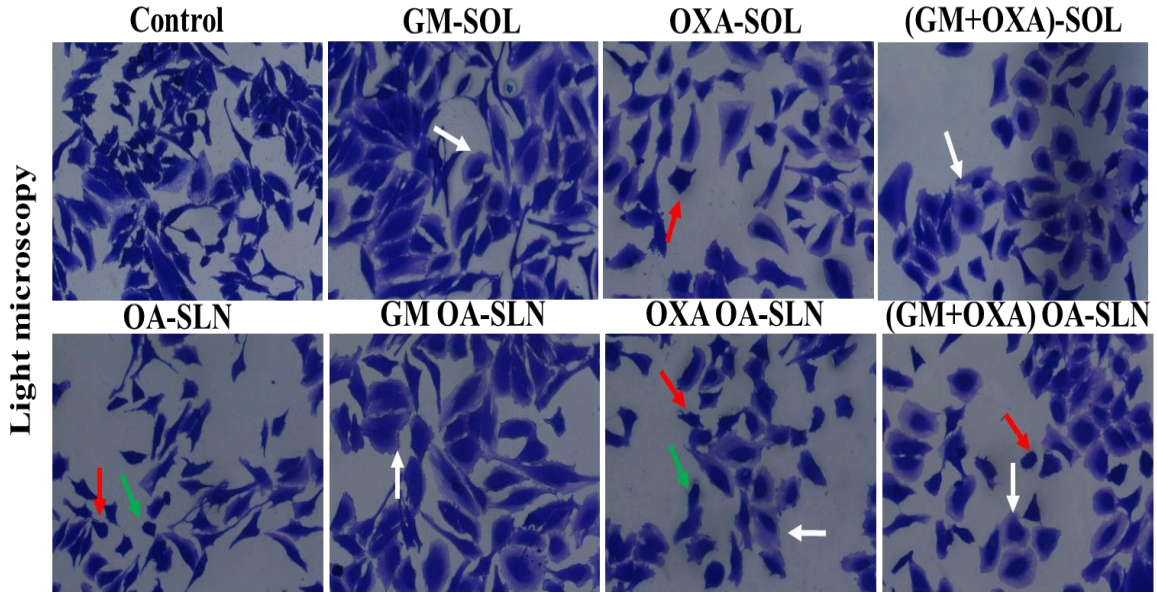


**Figure 3.** Morphological changes in the A549 cells. Cells were treated with different concentrations of tested formulas for 24 h. The changes observed as membrane blebbing (white arrow), chromatin condensation (red arrow), breaking up of the nucleus into discrete fragments (green arrow) in comparison to the control. Coomassie blue was used for staining, and images were taken at magnification 20×.

*3.4. Assessment of apoptotic activity via DAPI staining.*

The DAPI stain revealed the apoptotic nuclei that were identified by their distinctively marginated and fragmented appearance under the fluorescent microscope. After treatment with

different drug formulas for 24 h, a rise in the number of apoptotic nuclei and reduction in the area of the nuclei in the A549 cells treated with drug encapsulated OA-SLN compared to SOL-formula, and control was detected (Figure 4). It should be noted that blank OA-SLN has the most effect on A549 cells as most of the nuclei were destroyed.

*3.5. Cell apoptosis assessment.*

Cellular death may be determined by measuring the caspase-3 activity as a potential marker for apoptosis (Table 1). When A549 cells were incubated for 24 h with free drug and drug encapsulated OA-SLN and blank OA-SLN, the caspase-3 activities were increased by 1.01-fold and 1.10-fold after treatment with blank OA-SLN and GM OA-SLN, respectively compared with control cells. In contrast, other treatments did not induce significant apoptosis levels than those in control, thus limiting apoptosis induction.

*3.6. Assessment of A549 cellular death by autophagy.*

Cellular death can be through the autophagy pathway. After treatment with free drug and drug encapsulated OA-SLN and blank OA-SLN for 24 h, the level of LC3-B was measured by ELIZA as an indicator for autophagy.

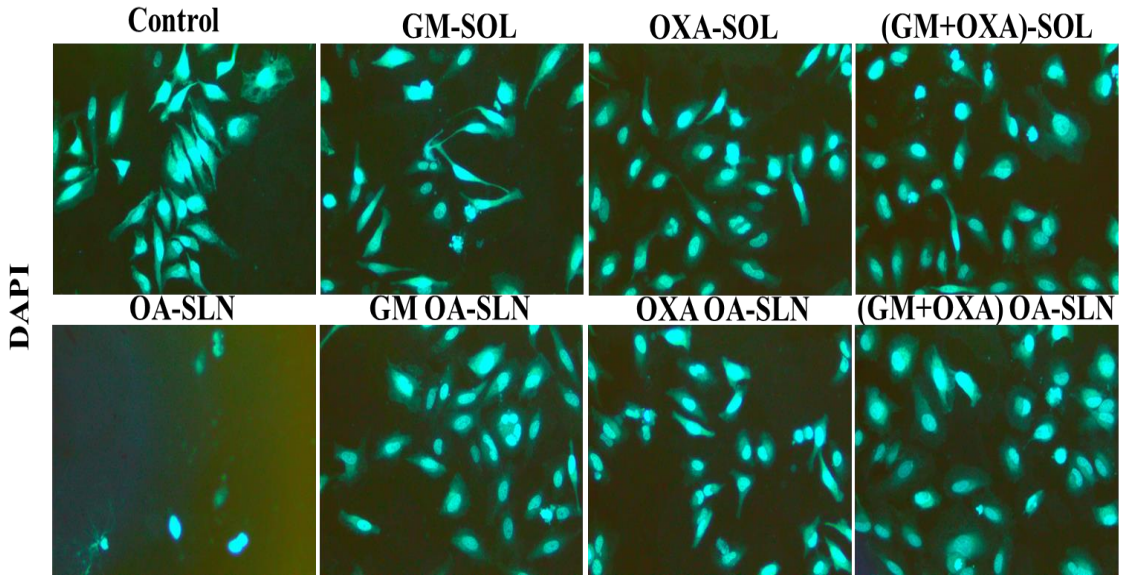


**Figure 4.** Fluorescent microscopy images of the A549 cells, stained with DAPI, at magnification 20×. Cells were treated with different concentrations of the tested formulas for 24 h.

**Table 1.** Cell apoptosis is determined by Caspase-3 activity measurement. The results were determined after 24 h incubation with different concentrations of the tested formulas. Data represent mean ± SD of two experiments.

| **Formula** | **Caspase 3 activity (% of activation)** | | | |
|---|---|---|---|---|
| | **Control** | **GM** | **OXA** | **(GEM+OXA)** |
| SOL | 100.00 ± 00 | 98.66 ± 2.54 | 99.84 ± 0.44 | 102.21 ± 2.38 |
| OA-SLN | 100.12 ± 2.09 | 100.96 ± 0.93 | 98.88 ± 2.46 | 100.40 ± 2.95 |

As demonstrated in Figure 5, the LC3-B concentration in A549 cells was significantly increased with treatment with blank OA-SLN (243.72 ± 2.60 pg/mL) compared to the untreated control cells (206.25 ± 6.69 pg/mL). Moreover, when A549 cells were treated with GM OA-SLN, there was a slight increase in LC3-B concentration (190.97 ± 6.96 pg/mL) compared to free GM-SOL (188.89 ± 3.57 pg/mL). However, the LC3-B concentration after OXA OA-SLN treatment was (161.80 ± 3.44 pg/mL) which was not significant when compared to the

untreated cells. In contrast, the combination treatment, (GM+OXA) OA-SLN, exhibited a significant increase in autophagy marker LC3-B (326.38 ± 4.21 pg/mL) when compared to the untreated cells.

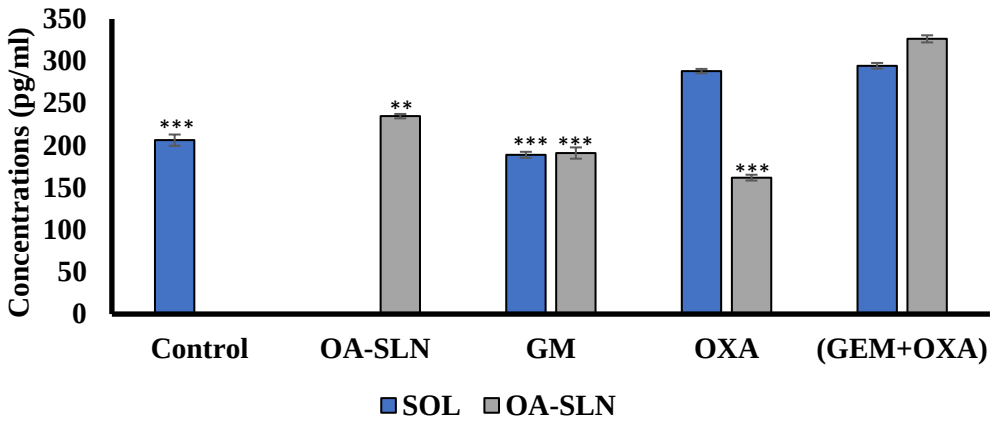


**Figure 5.** The effects of GM, OXA, OA-SLN, and their combinations on autophagy in A549 cells. ELISA assays were performed to examine the effects of different treatments on the level of the autophagy markers LC3-B in A549 cells after 24 h of treatment. ** = $p < 0.01$, *** = $p < 0.001$ vs (GM+OXA) OA-SLN. Data represent mean ± SD of two experiments.

Lung cancer is one of the deadliest types of malignancy worldwide, with poor response to conventional treatments and presents serious resistance to classical chemotherapy, leading to a high mortality rate [21]. A nano-drug delivery system to the lung cancer tumor mass may decrease the associated systemic adverse effects with conventional chemotherapeutic and increase the response rates [22]. This study aimed to design OA-based SLN to be a drug carrier to enhanced distribution to the target site, increase efficacy, and reduce the side effects. Also, the physical characteristics, *in vitro* cytotoxicity, and mechanism of cell death using the A549 cell line were evaluated.

In this study, the resulted homogenized OA-SLN was physically characterized by the dynamic light scattering techniques. The diameters of all formulas ranged from 63 to 200 nm. It has been reported that the nano-drug carrier with a particle size range of around 200 nm can be effectively delivered to tumor tissues [23]. Also, all formulas exhibited a relatively narrow size distribution (PDI < 1), which makes them mostly favorable for use in the drug delivery system. The zeta potential of all formulas was negative (< -10), which may be attributed to the carboxyl moiety of OA [24]. Negative charge nanoparticles are favorable because they have higher resistance to the droplets' coalescence and satisfy the stability requirement [25]. Also, Mucin in the lung's mucus layer is negatively charged, so the negatively charged nanoparticles facilely transport across the mucus barrier into the alveolar space with a pore size range of 60–300 nm, at which our nanoparticles in this study fell within this range [26].

Cytotoxicity screening by crystal violates revealed that blank OA-SLN and OXA encapsulated OA-SLN in single or combination have significantly lower $IC_{50}$ than the free drug. Similar to our result, other researchers reported that the anticancer activity of GM+OXA encapsulated in nanoparticles was improved significantly compared to the free drugs when subjected to different cancer cells [27, 28].

To investigate the mechanism of A549 cellular death, cells were stained with Coomassie blue dye. Furthermore, to examine the formula's ability to induce apoptosis, the nucleus was stained with DAPI, and caspase-3 activity was measured. The microscopical image showed that SLN formulas had induced more signs of apoptosis in A549 cells compared

to control and SOL-formulas. In fact, blank OA-SLN showed higher caspase-3 activities compared to control. This may be due to the small size of the nanoparticle formula (< 200 nm), leading to high cellular uptake by mucus layer of the lung and accumulation of the high amount of anticancer drug within alveolar space in the lung [29]. Moreover, the cytotoxic effect of the blank OA-SLN may be attributed to the negative charge caused by OA, leading to an increase in the permeability through the mucus layer of the lung cancer cell membrane [30].

GM and OXA drugs' effect and their combination in OA-SLN on autophagy pathways induction were further examined. It has been found that the induction of autophagy in A549 cells treated by blank OA-SLN was significant when compared to the untreated control as well as the combination treatment encapsulated (GM+OXA) OA-SLN. Similar to our finding, previous research demonstrated that cisplatin combined with graphene oxide–silver nanoparticle-induced autophagy and cellular death in the human ovarian carcinoma cells [31].

## 4. Conclusions

In the present study, an OA-based SLN was designed, synthesized, characterized, and evaluated *in vitro*. The cytotoxicity study revealed that OA-SLN and (GM+OXA) OA-SLN displayed significant cytotoxic and apoptotic effects on A549 cells when compared with the free SOL-formula and untreated control. OA-SLN and (GM+OXA) OA-SLN exert their cytotoxicity by induction of apoptosis, DNA damage, and autophagy, leading to lung cancer cellular death. Hence, OA-based nanoparticle provides a promising potential for drug delivery.

## Funding

This research received no external funding.

## Acknowledgments

The authors are deeply thankful to all of the Faculty and staff members in Regenerative Medicine, Immunology and Serology Units at King Fahd Medical Research Center, King Abdulaziz University, for their kind help and support.

## Conflicts of Interest

The authors declare no conflict of interest.

## References

1. Singh, R.; Peng, S.; Viswanath, P.; Sambandam, V.; Shen, L.; Rao, X.; Fang, B.; Wang, J.; Johnson, F. Non-canonical cM et regulation by vimentin mediates Plk1 inhibitor–induced apoptosis. *EMBO Mol Med* **2019**, *11*, 9960, https://doi.org/10.15252/emmm.201809960.
2. Maly, V.; Maly, O.; Kolostova, K.; Bobek, V. Circulating Tumor Cells in Diagnosis and Treatment of Lung Cancer. *In Vivo* **2019**, *33*, 1027-1037, https://doi.org/10.21873/invivo.11571.
3. Bossche, J.; Deben, C.; De Pauw, I.; Lambrechts, H.; Hermans, C.; Deschoolmeester, V.; Jacobs, J.; Specenier, P.; Pauwels, P.; Vermorken, J.; Peeters, M.; Lardon, F.; Wouters, A. In vitro study of the Polo-like kinase 1 inhibitor volasertib in non-small-cell lung cancer reveals a role for the tumor suppressor p53. *Mol Oncol* **2019**, *13*, 1196-1213, https://doi.org/10.1002/1878-0261.12477.
4. Beck, T.; Boumber, Y.; Aggarwal, C.; Pei, J.; Thrash-Bingham, C.; Fittipaldi, P.; Vlasenkova, R.; Rao, C.; Borghaei, H.; Cristofanilli, M.; Mehra, R.; Serebriiskii, I.; Alpaugh, R. Circulating tumor cell and cell-free RNA capture and expression analysis identify platelet-associated genes in metastatic lung cancer. *BMC Cancer* **2019**, *19*, 603, https://doi.org/10.1186/s12885-019-5795-x.

5. Alven, S.; Aderibigbe, B. Efficacy of Polymer-Based Nanocarriers for Co-Delivery of Curcumin and Selected Anticancer Drugs. *Nanomaterials* **2020**, *10*, 1556, https://doi.org/10.3390/nano10081556.
6. Nair, A.; Shah, J.; Al-Dhubiab, B.; Patel, S.; Morsy, M.; Patel, V.; Chavda, V.; Jacob, S.; Sreeharsha, N.; Shinu, P.; Attimarad, M.; Venugopala, K. Development of asialoglycoprotein receptor-targeted nanoparticles for selective delivery of gemcitabine to hepatocellular carcinoma. *Molecules* **2019**, *24*, 4566, https://doi.org/10.3390/molecules24244566.
7. Liu, W., Mao, Y., Zhang, X., Wang, Y., Wu, J., Zhao, S., Peng, S., Zhao, M. RGDV-modified gemcitabine: a nano-medicine capable of prolonging half-life, overcoming resistance and eliminating bone marrow toxicity of gemcitabine. *Int J Nanomedicine* **2019**, *14*, 7263–7279, https://doi.org/10.2147/IJN.S212978.
8. Tang, Z., Feng, W., Yang, Y., Wang, Q. Gemcitabine-loaded RGD modified liposome for ovarian cancer: preparation, characterization and pharmacodynamic studies. *Drug Des Devel Ther* **2019**, *13*, 3281–3290, https://doi.org/10.2147/DDDT.S211168.
9. Wang, Y., Zhang, X., Zhang, W., Dong, H., Zhang, W., Mao, J., Dai, Y. Combination of oxaliplatin and Vit.E-TPGS in lipid nanosystem for enhanced therapeutic efficacy in colon cancers. *Pharm Res* **2018**, *35*, 27, https://doi.org/10.1007/s11095-017-2297-x.
10. Conteduca, V., Gurioli, G., Rossi, L., Scarpi, E., Lolli, C., Schepisi, G., Farolfi, A., De Lisi, D., Gallà, V., Burgio, S. L., Menna, C., Amadori, A., Losi, L., Amadori, D., Costi, M. P., De Giorgi, U. Oxaliplatin plus leucovorin and 5-fluorouracil (FOLFOX-4) as a salvage chemotherapy in heavily-pretreated platinum-resistant ovarian cancer. *BMC Cancer* **2018**, *18*, 1267, https://doi.org/10.1186/s12885-018-5180-1.
11. Kadina, Y. A., Razuvaeva, E. V., Streltsov, D. R., Sedush, N. G., Shtykova, E. V., Kulebyakina, A. I., Puchkov, A. A., Volkov, D. S., Nazarov, A. A., Chvalun, S. N. Poly(Ethylene Glycol)-b-Poly(D,L-Lactide) nanoparticles as potential carriers for anticancer drug oxaliplatin. *Molecules* **2021**, *26*, 602, https://doi.org/10.3390/molecules26030602.
12. Caballero, A. B., Cardo, L., Claire, S., Craig, J. S., Hodges, N. J., Vladyka, A., Albrecht, T., Rochford, L. A., Pikramenou, Z., Hannon, M. J. Assisted delivery of anti-tumour platinum drugs using DNA-coiling gold nanoparticles bearing lumophores and intercalators: towards a new generation of multimodal nanocarriers with enhanced action. *Chem Sci* **2019**, *10*, 9244–9256, https://doi.org/10.1039/c9sc02640a.
13. Parvez, S., Yadagiri, G., Gedda, M. R., Singh, A., Singh, O. P., Verma, A., Sundar, S., Mudavath, S. L. Modified solid lipid nanoparticles encapsulated with Amphotericin B and Paromomycin: an effective oral combination against experimental murine visceral leishmaniasis. *Sci Rep* **2020**, *10*, 12243, https://doi.org/10.1038/s41598-020-69276-5.
14. Wang, H., Li, L., Ye, J., Wang, R., Wang, R., Hu, J., Wang, Y., Dong, W., Xia, X., Yang, Y., Gao, Y., Gao, L., Liu, Y. Improving the oral bioavailability of an anti-glioma prodrug CAT3 using novel solid lipid nanoparticles containing oleic acid-CAT3 conjugates. *Pharmaceutics* **2020**, *12*, 126, https://doi.org/10.3390/pharmaceutics12020126.
15. Lim, J. H., Gerhart-Hines, Z., Dominy, J. E., Lee, Y., Kim, S., Tabata, M., Xiang, Y. K., Puigserver, P. Oleic acid stimulates complete oxidation of fatty acids through protein kinase A-dependent activation of SIRT1-PGC1α complex. *J Biol Chem* **2013**, *288*, 7117–7126, https://doi.org/10.1074/jbc.M112.415729.
16. Rath, E. M., Cheng, Y. Y., Pinese, M., Sarun, K. H., Hudson, A. L., Weir, C., Wang, Y. D., Håkansson, A. P., Howell, V. M., Liu, G. J., Reid, G., Knott, R. B., Duff, A. P., Church, W. B. BAMLET kills chemotherapy-resistant mesothelioma cells, holding oleic acid in an activated cytotoxic state. *PLoS One* **2018**, *13*, 0203003, https://doi.org/10.1371/journal.pone.0203003.
17. Wang, X., Yu, B., Ren, W., Mo, X., Zhou, C., He, H., Jia, H., Wang, L., Jacob, S. T., Lee, R. J., Ghoshal, K., Lee, L. J. Enhanced hepatic delivery of siRNA and microRNA using oleic acid based lipid nanoparticle formulations. *J Control Release* **2013**, *172*, 690–698, https://doi.org/10.1016/j.jconrel.2013.09.027.
18. Alkhatib, M. H., Alyamani, S. A., Abdu, F. Incorporation of methotrexate into coconut oil nanoemulsion potentiates its antiproliferation activity and attenuates its oxidative stress. *Drug Deliv* **2020**, *27*, 422–430, https://doi.org/10.1080/10717544.2020.1736209.
19. Alkhatib, M. H., Al-Otaibi, W. A., Wali, A. N. Antineoplastic activity of mitomycin C formulated in nanoemulsions-based essential oils on HeLa cervical cancer cells. *Chem Biol Interact* **2018**, *291*, 72–80, https://doi.org/10.1016/j.cbi.2018.06.009.
20. Du, J., Li, J., Song, D., Li, Q., Li, L., Li, B., Li, L. Matrine exerts anti-breast cancer activity by mediating apoptosis and protective autophagy via the AKT/mTOR pathway in MCF-7 cells. *Mol Med Rep* **2020**, *22*, 3659–3666, https://doi.org/10.3892/mmr.2020.11449.

21. Andey, T., Bora-Singhal, N., Chellappan, S. P., Singh, M. Cationic lipoplexes for treatment of cancer stem cell-derived murine lung tumors. *Nanomedicine: Nanotechnology, Biology and Medicine* **2019**, *18*, 31–43, https://doi.org/10.1016/j.nano.2019.02.007.
22. Youngren-Ortiz, S. R., Hill, D. B., Hoffmann, P. R., Morris, K. R., Barrett, E. G., Forest, M. G., Chougule, M. B. Development of optimized, inhalable, gemcitabine-loaded gelatin nanocarriers for lung cancer. *J Aerosol Med Pulm Drug Deliv* **2017**, *30*, 299–321, https://doi.org/10.1089/jamp.2015.1286.
23. Zhang, W., Xu, W., Lan, Y., He, X., Liu, K., Liang, Y. Antitumor effect of hyaluronic-acid-modified chitosan nanoparticles loaded with siRNA for targeted therapy for non-small cell lung cancer. *Int J Nanomedicine* **2019**, *14*, 5287–5301, https://doi.org/10.2147/IJN.S203113.
24. Zhao, H., Lu, H., Gong, T., Zhang, Z. Nanoemulsion loaded with lycobetaine-oleic acid ionic complex: physicochemical characteristics, in vitro, in vivo evaluation, and antitumor activity. *Int J Nanomedicine* **2013**, *8*, 1959–1973, https://doi.org/10.2147/IJN.S43892.
25. Chen, C. Y., Lee, Y. H., Chang, S. H., Tsai, Y. F., Fang, J. Y., Hwang, T. L. Oleic acid-loaded nanostructured lipid carrier inhibit neutrophil activities in the presence of albumin and alleviates skin inflammation. *Int J Nanomedicine* **2019**, *14*, 6539–6553, https://doi.org/10.2147/IJN.S208489.
26. Yu, H. P., Liu, F. C., Umoro, A., Lin, Z. C., Elzoghby, A. O., Hwang, T. L., Fang, J. Y. Oleic acid-based nanosystems for mitigating acute respiratory distress syndrome in mice through neutrophil suppression: how the particulate size affects therapeutic efficiency. *J Nanobiotechnology* **2020**, *18*, 25, https://doi.org/10.1186/s12951-020-0583-y.
27. Poon, C., He, C., Liu, D., Lu, K., Lin, W. Self-assembled nanoscale coordination polymers carrying oxaliplatin and gemcitabine for synergistic combination therapy of pancreatic cancer. *J Control Release* **2015**, *201*, 90–99, https://doi.org/10.1016/j.jconrel.2015.01.026.
28. Ye, H., Tong, J., Liu, J., Lin, W., Zhang, C., Chen, K., Zhao, J., Zhu, W. Combination of gemcitabine-containing magnetoliposome and oxaliplatin-containing magnetoliposome in breast cancer treatment: A possible mechanism with potential for clinical application. *Oncotarget* **2016**, *7*, 43762–43778, https://doi.org/10.18632/oncotarget.9671.
29. Alkhatib, M. H., Aljadani, M. A., Mahassni, S. H. Carrying epirubicin on nanoemulsion containing algae and cinnamon oils augments its apoptotic and anti-invasion effects on human colon cancer cells. *Am J Transl Res* **2020**, *12*, 2463–2472.
30. Zhang, R., Ru, Y., Gao, Y., Li, J., Mao, S. Layer-by-layer nanoparticles co-loading gemcitabine and platinum (IV) prodrugs for synergistic combination therapy of lung cancer. *Drug Des Devel Ther* **2017**, *11*, 2631–2642, https://doi.org/10.2147/DDDT.S143047.
31. Yuan, Y. G., Gurunathan, S. Combination of graphene oxide-silver nanoparticle nanocomposites and cisplatin enhances apoptosis and autophagy in human cervical cancer cells. *Int J Nanomedicine* **2017**, *12*, 6537–6558, https://doi.org/10.2147/IJN.S125281.